DIGITAL FILTER INITIALIZATION

PETER LYNCH
Met Éireann,
Glasnevin Hill, Dublin 9, Ireland.

1. Introduction

The requirement to modify meteorological analyses to avoid spurious high frequency oscillations in numerical forecasts has been known from the beginning of numerical weather prediction. The most popular method of initialization up to recently was normal mode initialization, or NMI (Machenhauer, 1977). This has been used in many NWP centres, and has performed satisfactorily. Its most natural context is for global models, for which the horizontal structure of the normal modes corresponds to the Hough functions, the eigenmodes of the Laplace Tidal Equations. For limited area models, normal modes can also be derived, but the lateral boundaries force the introduction of simplifying assumptions.

Recently, an alternative method of initialization, called digital filter initialization (DFI), was introduced by Lynch and Huang (1992). It was generalised to allow for diabatic effects by Huang and Lynch (1993). The latter paper also discussed the use of an optimal filter. A much simpler filter, the Dolph-Chebyshev filter, which is a special case of the optimal filter, was applied to the initialization problem by Lynch (1997). A more efficient formulation of DFI was presented by Lynch, Giard and Ivanovici (1997).

2. Advantages of DFI

The method of digital filter initialization, which is based on ideas from digital signal processing, has significant advantages over alternative methods, and is now in use operationally at several major weather prediction centres. Some of the principal advantages of DFI compared to available alternatives are:

1. No need to compute or store normal modes;
2. No need to separate vertical modes;
3. Complete compatibility with model discretisation;
4. Applicable to exotic grids on arbitrary domains;

5. No iterative numerical procedure which may diverge;
6. Ease of implementation and maintenance, due to simplicity of scheme;
7. Applicable to all prognostic model variables;
8. Applicable to non-hydrostatic models.

The first advantage becomes more pronounced as the number of degrees of freedom of the model increases. The second advantage over NMI is that the latter method requires the introduction of an auxiliary geopotential variable, and partitioning of its changes between the temperature and surface pressure involves an *ad hoc* assumption. Advantage 3 eliminates discretization errors due to grid disparities. Advantage 4 facilitates the use of stretched or irregular model grids. Advantage 5 means that all the vertical modes can be initialized effectively. The sixth advantage is that the simplicity of the method makes it easy to implement and maintain. The seventh is that additional prognostic model variables, such as cloud water, rain water, turbulent kinetic energy, etc., are processed in the same way as the standard mass and wind variables; thus, DFI produces initial fields for these variables which are compatible with the basic dynamical fields. Last but not least, DFI filters the additional prognostic variables in non-hydrostatic models in a manner identical to the basic variables. The DFI method is thus immediately suitable for non-hydrostatic models (Bubnová, *et al.*, 1995). This is not the case for NMI. It must be pointed out that DFI is significantly more demanding of computational time than NMI. However, the significant benefits justify this additional cost.

3. The Primitive Notion of Filtering

The concept of filtering has a rôle in virtually every field of study, from topology to theology, seismology to sociology. The process of filtering involves the *selection* of those components of an assemblage having some particular property, and the removal or elimination of those components which lack it. A filter is any device or contrivance designed to carry out such a selection. It may be represented by a simple system diagram, having an input with both desired and undesired components, and an output comprising only the former.

We are primarily concerned with filters as used in signal processing. The selection principle for these is generally based on the frequency of the signal components. There are a number of ideal types — lowpass, highpass, bandpass and bandstop — corresponding to the range of frequencies which pass through the filter and those which are rejected. In many cases the input consists of a low-frequency (LF) signal contaminated by high-frequency (HF) noise, and the information in the signal can be isolated by using a

lowpass filter which rejects the noise. Such a situation is typical for the application to meteorology discussed below.

Filter theory originated from the need to design electronic circuits with precise frequency-selective characteristics, for radio and telecommunications. These analog filters were constructed from capacitors and inductors, and acted on continuous time signals. More recently, discrete time signal processing has assumed prominence, and the technique and theory of *digital filtering* has evolved. Digital filters may be implemented in hardware using integrated circuits, but are more commonly realized in software: the input is processed by a program designed to perform the required selection and compute the output.

4. Nonrecursive and Recursive Digital Filters

Given a discrete function of time, $\{x_n\}$, a *nonrecursive* digital filter is defined by

$$y_n = \sum_{k=-N}^{N} a_k x_{n-k}. \tag{1}$$

The output y_n at time $n\Delta t$ depends on both past and future values of x_n, but not on other output values. A *recursive* digital filter is defined by

$$y_n = \sum_{k=K}^{N} a_k x_{n-k} + \sum_{k=1}^{L} b_k y_{n-k} \tag{2}$$

where K, L and N are integers, with L and N positive. The output y_n at time $n\Delta t$ in this case depends on past and present values of the input (for $K = 0$), and also on previous output values (occasionally, future input values are also used ($K < 0$), in which case the recursive filter is *non-causal*). Recursive filters are more powerful than non-recursive ones, but can also be more problematical, as the feedback of the output can give rise to instability. The response of a nonrecursive filter to an impulse $\delta(n)$ is zero for $|n| > N$, giving rise to the alternative name *finite impulse response* or FIR filter. Since the response of a recursive filter to this input can persist indefinitely, it is known as an *infinite impulse response* or IIR filter.

The frequency response of a recursive filter is easily found: let $x_n = \exp(in\theta)$ and assume an output of the form $y_n = H(\theta)\exp(in\theta)$; substituting into (2), the transfer function $H(\theta)$ is

$$H(\theta) = \frac{\sum_{k=K}^{N} a_k e^{-ik\theta}}{1 - \sum_{k=1}^{L} b_k e^{-ik\theta}}. \tag{3}$$

For nonrecursive filters the denominator reduces to unity. This equation gives the response once the filter coefficients a_k and b_k have been specified.

However, what is really required is the opposite: to derive coefficients (and as few as possible) which will yield the desired response function. This *inverse problem* has no unique solution, and a great variety of techniques have been developed.

Only the most elementary design techniques for non-recursive filters will be considered below. Recursive filters generally have superior performance to nonrecursive filters with the same total number of coefficients. Numerous accounts of recursive digital filters are available in publications on digital signal processing (*e.g.*, Oppenheim and Schafer, 1989). For a review in the meteorological literature, see Raymond (1988), where another class of filter, the implicit filter, is also discussed.

5. Design of Nonrecursive Filters

Consider a function of time, $f(t)$, with low and high frequency components. To filter out the high frequencies one may proceed as follows:

[1] Calculate the Fourier transform $F(\omega)$ of $f(t)$;
[2] Set the coefficients of the high frequencies to zero;
[3] Calculate the inverse transform.

Step [2] may be performed by multiplying $F(\omega)$ by an appropriate weighting function $H_c(\omega)$. Typically, $H_c(\omega)$ is a step function

$$H_c(\omega) = \begin{cases} 1, & |\omega| \leq |\omega_c|; \\ 0, & |\omega| > |\omega_c|, \end{cases} \tag{4}$$

where ω_c is a cutoff frequency. These three steps are equivalent to a convolution of $f(t)$ with $h(t) = \sin(\omega_c t)/\pi t$, the inverse Fourier transform of $H_c(\omega)$. This follows from the convolution theorem

$$\mathcal{F}\{(h * f)(t)\} = \mathcal{F}\{h\} \cdot \mathcal{F}\{f\} = H_c(\omega) \cdot F(\omega) \tag{5}$$

Thus, to filter $f(t)$ one calculates

$$f^\star(t) = (h * f)(t) = \int_{-\infty}^{+\infty} h(\tau) f(t - \tau) d\tau. \tag{6}$$

For simple functions $f(t)$, this integral may be evaluated analytically. In general, some method of approximation must be used.

Suppose now that f is known only at discrete moments $t_n = n\Delta t$, so that the sequence $\{\cdots, f_{-2}, f_{-1}, f_0, f_1, f_2, \cdots\}$ is given. For example, f_n could be the value of some model variable at a particular grid point at time t_n. The shortest period component which can be represented with a time step Δt is $\tau_N = 2\Delta t$, corresponding to a maximum frequency, the so-called Nyquist frequency, $\omega_N = \pi/\Delta t$. The sequence $\{f_n\}$ may be regarded as the Fourier coefficients of a function $F(\theta)$:

$$F(\theta) = \sum_{n=-\infty}^{\infty} f_n e^{-in\theta}, \tag{7}$$

where $\theta = \omega\Delta t$ is the *digital frequency* and $F(\theta)$ is periodic, $F(\theta) = F(\theta + 2\pi)$. High frequency components of the sequence may be eliminated by multiplying $F(\theta)$ by a function $H_d(\theta)$ defined by

$$H_d(\theta) = \begin{cases} 1, & |\theta| \leq |\theta_c|; \\ 0, & |\theta| > |\theta_c|, \end{cases} \tag{8}$$

where the cutoff frequency $\theta_c = \omega_c \Delta t$ is assumed to fall in the Nyquist range $(-\pi, \pi)$ and $H_d(\theta)$ has period 2π. This function may be expanded:

$$H_d(\theta) = \sum_{n=-\infty}^{\infty} h_n e^{-in\theta} \qquad ; \qquad h_n = \frac{1}{2\pi} \int_{-\pi}^{\pi} H_d(\theta) e^{in\theta} d\theta. \tag{9}$$

The values of the coefficients h_n follow immediately from (8) and (9):

$$h_n = \frac{\sin n\theta_c}{n\pi}. \tag{10}$$

Let $\{f_n^\star\}$ denote the low frequency part of $\{f_n\}$, from which all components with frequency greater than θ_c have been removed. Clearly,

$$H_d(\theta) \cdot F(\theta) = \sum_{n=-\infty}^{\infty} f_n^\star e^{-in\theta}.$$

The convolution theorem for Fourier series now implies that $H_d(\theta) \cdot F(\theta)$ is the transform of the convolution of $\{h_n\}$ with $\{f_n\}$:

$$f_n^\star = (h * f)_n = \sum_{k=-\infty}^{\infty} h_k f_{n-k}. \tag{11}$$

This enables the filtering to be performed directly on the given sequence $\{f_n\}$. It is the discrete analogue of (6). In practice the summation must be truncated at some finite value of k. Thus, an approximation to the low frequency part of $\{f_n\}$ is given by

$$f_n^\star = \sum_{k=-N}^{N} h_k f_{n-k}. \tag{12}$$

Comparing (12) with (1), it is apparent that the finite approximation to the discrete convolution is formally identical to a nonrecursive digital filter.

As is well known, truncation of a Fourier series gives rise to Gibbs oscillations. These may be greatly reduced by means of an appropriately defined "window" function. The response of the filter is improved if h_n is multiplied by the Lanczos window

$$w_n = \frac{\sin(n\pi/(N+1))}{n\pi/(N+1)}.$$

The transfer function $H(\theta)$ of a filter is defined as the function by which a pure sinusoidal oscillation is multiplied when subjected to the filter. For symmetric coefficients, $h_k = h_{-k}$, it is real, implying that the phase is not altered by the filter. Then, if $f_n = \exp(in\theta)$, one may write $f_n^\star = H(\theta) \cdot f_n$, and $H(\theta)$ is easily calculated by substituting f_n in (12):

$$H(\theta) = \sum_{k=-N}^{N} h_k e^{-ik\theta} = \left[h_0 + 2 \sum_{k=1}^{N} h_k \cos k\theta \right]. \tag{13}$$

The transfer functions for a windowed and unwindowed filter are shown in Lynch and Huang (1992, Fig. 2). The use of the window decreases the Gibbs oscillations in the stop-band $|\theta| > |\theta_c|$. However, it also has the effect of widening the pass-band beyond the nominal cutoff. For a fuller discussion of windowing see *e.g.* Hamming (1989) or Oppenheim and Schafer (1989).

One of the simplest design methods for nonrecursive filters is the expansion of the desired filtering function, $H(\theta)$, as a Fourier series, and the application of a suitable window function to improve the transfer characteristics. That is the method employed above. An alternative method called frequency sampling fits the desired frequency response by making a selection of values and calculating the inverse discrete Fourier transform to obtain the filter coefficients. A more sophisticated method uses the Chebyshev alternation theorem to obtain a filter whose maximum error in the pass- and stop-bands is minimized. This method yields a filter meeting required specifications with fewer coefficients that the other methods. The design of nonrecursive and recursive filters is outlined in Hamming (1989), where several methods are described, and fuller treatments may be found in Oppenheim and Schafer (1989).

6. Application of a Nonrecursive Digital Filter to Initialization

An initialization scheme using a nonrecursive digital filter has been developed by Lynch and Huang (1992) for the HIRLAM model. The value chosen for the cutoff frequency corresponded to a period $\tau_c = 6$ hours. With the time step $\Delta t = 6$ minutes used in the model, this corresponds to a (digital) cutoff frequency $\theta_c = \pi/30$. The coefficients were derived by Fourier expansion of a step-function, truncated at $N = 30$, with application of a Lanczos window, and are given by

$$h_n = \left[\frac{\sin(n\pi/(N+1))}{n\pi/(N+1)} \right] \left(\frac{\sin(n\theta_c)}{n\pi} \right).$$

The frequency response was depicted in Lynch and Huang (1992, Fig. 2). The central lobe of the coefficient function spans a period of six hours, from $t = -3$ hours to $t = +3$ hours. The summation in (1) was calculated over this range, with the coefficients normalized to have unit sum over the span.

Thus, the application of the technique involved computation equivalent to sixty time steps, or a six hour adiabatic integration.

The uninitialized fields of surface pressure, temperature, humidity and winds were first integrated forward for three hours, and running sums of the form

$$f_F^\star(0) = \frac{1}{2}h_0 f_0 + \sum_{n=1}^{N} h_{-n} f_n, \tag{14}$$

where $f_n = f(n\Delta t)$, were calculated for each field at each gridpoint and on each model level. These were stored at the end of the three hour forecast. The original fields were then used to make a three hour 'hindcast', during which running sums of the form

$$f_B^\star(0) = \frac{1}{2}h_0 f_0 + \sum_{n=-1}^{-N} h_{-n} f_n \tag{15}$$

were accumulated for each field, and stored as before. The two sums were then combined to form the required summations:

$$f^\star(0) = f_F^\star(0) + f_B^\star(0). \tag{16}$$

These fields correspond to the application of the digital filter (1) to the original data, and will be referred to as the filtered data.

In the foregoing, only the amplitudes of the transfer functions have been discussed. Since these functions are complex, there is also a phase change induced by the filters. Space prohibits further discussion here; however, it is essential that the phase characteristics of a filter be studied before it is considered for use. Ideally, the phase-error should be as small as possible for the low frequency components which are meteorologically important. The error in the high frequency stop-band is unimportant. It is salutary to recall that phase-errors are amongst the most prevalent and pernicious problems faced by the forecaster.

7. The Dolph-Chebyshev Filter

We now consider a particularly simple filter, having explicit expressions for its impulse response coefficients. The details of the Dolph-Chebyshev filter are presented in Lynch (1997). We will confine the present discussion to the definition and principal properties of the filter; further information may be found in the reference cited.

7.1. DEFINITION OF THE FILTER

The function to be described is constructed using Chebyshev polynomials, defined by the equations

$$T_n(x) = \begin{cases} \cos(n\cos^{-1}x), & \text{if } |x| \le 1; \\ \cosh(n\cosh^{-1}x), & \text{if } |x| > 1. \end{cases}$$

Clearly, $T_0(x) = 1$ and $T_1(x) = x$. From the definition, the following recurrence relation follows immediately:

$$T_n(x) = 2xT_{n-1}(x) - T_{n-2}(x), \quad n \geq 2.$$

The main relevant properties of these polynomials are given in Lynch (1997).

Now consider the function defined in the frequency domain by

$$H(\theta) = \frac{T_{2M}\left(x_0 \cos\left(\theta/2\right)\right)}{T_{2M}(x_0)}$$

where $x_0 > 1$. Let θ_s be such that $x_0 \cos(\theta_s/2) = 1$. As θ varies from 0 to θ_s, $H(\theta)$ falls from 1 to $r = 1/T_{2M}(x_0)$. For $\theta_s \leq \theta \leq \pi$, $H(\theta)$ oscillates in the range $\pm r$. The form of $H(\theta)$ is that of a low-pass filter with a cut-off at $\theta = \theta_s$. By means of the definition of $T_n(x)$ and basic trigonometric identities, $H(\theta)$ can be written as a *finite expansion*

$$H(\theta) = \sum_{n=-M}^{+M} h_n \exp(-in\theta).$$

The coefficients $\{h_n\}$ may be evaluated from the inverse Fourier transform

$$h_n = \frac{1}{N}\left[1 + 2r \sum_{m=1}^{M} T_{2M}\left(x_0 \cos\frac{\theta_m}{2}\right) \cos m\theta_n\right],$$

where $|n| \leq M$, $N = 2M + 1$ and $\theta_m = 2\pi m/N$ (Antoniou, 1993). Since $H(\theta)$ is real and even, h_n are also real and $h_{-n} = h_n$. The weights $\{h_n : -M \leq n \leq +M\}$ define the Dolph-Chebyshev or, for short, Dolph filter.

In the HIRLAM model, the filter order $N = 2M + 1$ is determined by the time step Δt and forecast span T_S. The desired frequency cut-off is specified by choosing a value for the cut-off period, τ_s. Then $\theta_s = 2\pi\Delta t/\tau_s$ and the parameters x_0 and r are given by

$$\frac{1}{x_0} = \cos\frac{\theta_s}{2}, \quad \frac{1}{r} = \cosh\left(2M \cosh^{-1} x_0\right).$$

The ripple ratio r is a measure of the maximum amplitude in the stop-band $[\theta_s, \pi]$: r = [side-lobe amplitude/main-lobe amplitude]. The Dolph filter has minimum ripple-ratio for given main-lobe width and filter order.

7.2. AN EXAMPLE OF THE DOLPH FILTER

Let us suppose components with period less than three hours are to be eliminated ($\tau_s = 3\,\mathrm{h}$) and the time step is $\Delta t = \frac{1}{2}\,\mathrm{h}$. Then $\theta_s = 2\pi\Delta t/\tau_s \approx 1.05$. It can be shown that a filter of order $N = 7$, or span $T = 2M\Delta t = 3\,\mathrm{h}$, attenuates high frequency components by more than 20 dB (the attenuation in the stop-band is $\delta = 20\log_{10}|H(\theta)|$). This level of damping implies that

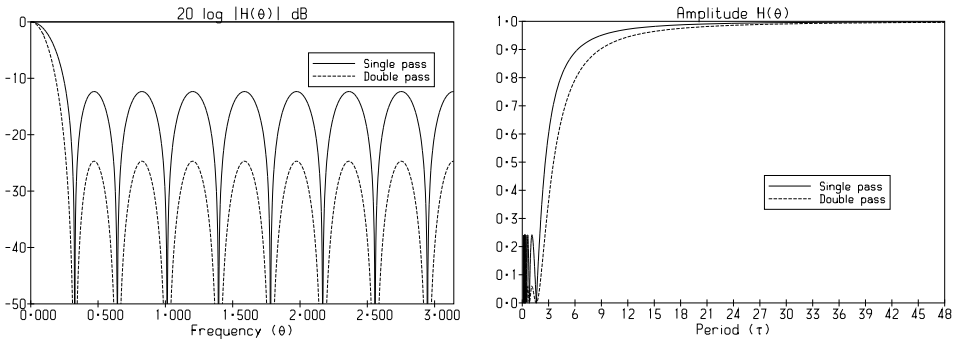

Fig. 1. Frequency response for Dolph filter with span $T_S = 2$h, order $N = 2M + 1 = 17$ and cut-off $\tau_s = 3$h. Results for single and double application are shown. Left: Logarithmic response (dB) as a function of frequency. Right: Amplitude response as a function of period.

the amplitudes of high-frequency components are reduced by at least 90% and their energy by at least 99%, which is found to be adequate in practice.

The DFI procedure employed in the HIRLAM model involves a double application of the filter. Thus, we examine both the frequency response $H(\theta)$ and its square, $H(\theta)^2$, as the effect of a second pass through the filter is to square the frequency response. The parameters chosen for the DFI tests below are span $T_S = 2\,\mathrm{h}$, cut-off period $\tau_s = 3\,\mathrm{h}$ and time step $\Delta t = 450\,\mathrm{s} = \frac{1}{8}\,\mathrm{h}$. So, $M = 8$, $N = 17$ and $\theta_s = 2\pi\Delta t/\tau_s \approx 0.26$. The response and square response are shown in Fig. 1 (left panel). The ripple ratio has the value $r = 0.241$. A single pass attenuates high frequencies (components with $|\theta| > |\theta_s|$) by at least 12.4dB. For a double pass, the minimum attenuation is about 25dB, more than adequate for elimination of HF noise. For ease of visualisation, the response is also plotted as a function of period in Fig. 1 (right panel). From this it is clear that the amplitudes of components with periods less than two hours are reduced to less than 5% of their original value. At the same time, components with periods greater than one day are substantially left unchanged. It is crucial for an initialization scheme that it does not distort the meteorologically significant components of the flow: the filter described here has the required property.

In Lynch (1997, Appendix) it is proved that the Dolph window is an *optimal* filter whose pass-band edge, θ_p, is the solution of the equation $H(\theta) = 1 - r$. Since an optimal filter is, by construction, the best possible solution to minimizing the maximum deviation from the ideal in the pass- and stop-bands, the Dolph filter shares this property provided the equivalence holds. However, note the essential distinction: for the general optimal filter, θ_p can be freely chosen; for the Dolph window, it is determined by the other parameters. The algorithm for the optimal filter is complex, involving

about one thousand lines of code; calculation of the Dolph filter coefficients is trivial by comparison.

8. Implementation in HIRLAM

8.1. OUTLINE OF THE METHOD

The digital filter initialization is performed by applying the filter to time series of model variables. The coefficients of the Dolph filter, $\{h_n : -M \leq n \leq +M\}$, are real and symmetric: $h_{-n} = h_n$. Thus, the phase response is such that the output is valid at the centre of the span. If we had a model integration centred on the initial time, $t = 0$, the filter would produce output valid at that time. However, as the model contains irreversible physical processes, it is not possible to integrate it backwards in time. The solution is to apply the filter in two stages: in the first, a backward integration from $t = 0$ to $t = -T_S$ is performed, with all irreversible physics switched off. The filter output is calculated by accumulating sums of the form

$$\bar{x} = \sum_{n=0}^{n=N} h_{n-M} x_n \, ,$$

where x is a particular prognostic variable at a particular grid point and level (the same sum is accumulated for all prognostic variables). The output $\bar{x}$ is valid at time $t = -\frac{1}{2}T_S$. In the second stage, a forward integration is made from $t = -\frac{1}{2}T_S$ to $t = +\frac{1}{2}T_S$, starting from the output of the first stage. Once again, the filter is applied by accumulating sums formally identical to those of the first stage. But now the output is valid at the centre of the interval $[-\frac{1}{2}T_S, +\frac{1}{2}T_S]$, *i.e.*, at $t = 0$. The output of the second pass of the filter is the initialized data. The values of the prognostic variables at the lateral boundaries are left unchanged during the digital filtering process.

An adiabatic backward integration followed by a diabatic forward integration will not return the variables to their initial values. This deviation, called the diabatic discrepancy, is reduced by the method of Lynch, *et al.* (1997), but not completely eliminated. Some work towards developing a boundary filter, relying solely on a forward integration, is reported in Lynch and McGrath (2001).

Complete technical details of the original implementation of DFI in the HIRLAM model may be found in Lynch, *et al.*, (1999). A reformulation of the implementation, with further testing and evaluation, is presented in Huang and Yang, 2002.

8.2. INITIALIZATION EXAMPLE

A detailed case study based on the first implementation in HIRLAM was carried out to check the effect of the initialization on the initial fields and on the forecast, and to examine the efficacy of DFI in eliminating high frequency noise. The digital filter initialization was compared to the reference

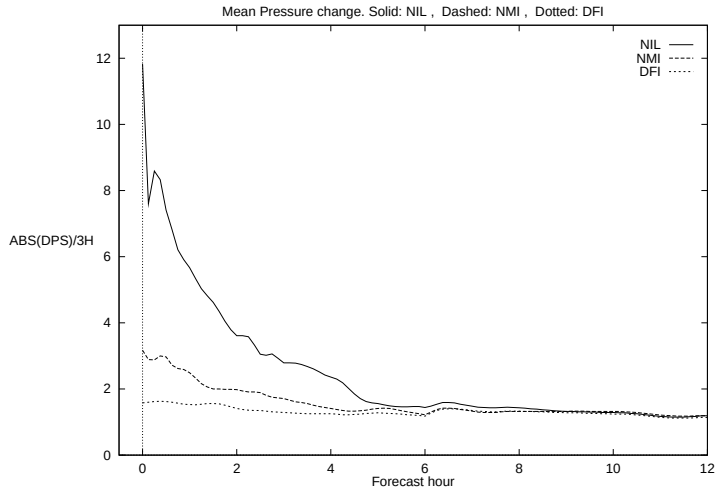

Fig. 2. Mean absolute surface pressure tendency for three forecasts. Solid: uninitialized analysis (NIL). Dashed: Normal mode initialization (NMI). Dotted: Digital filter initialization (DFI). Units are hPa/3 hours.

implicit normal mode initialization (NMI) scheme, and to forecasts with no initialization (NIL). Forecasts starting from the analysis valid at 1200 UTC on 10 February, 1999 were compared.

We first checked the effect of DFI on the analysis and forecast fields. The maximum change in surface pressure is 2.2hPa, with an *rms* change of about 0.5hPa. The changes to the other analysed variables are in general comparable in size to analysis errors, and considerably smaller in magnitude than typical changes brought about by the analysis itself: the *rms* change in surface pressure from first-guess to analysis is about 1hPa. The *rms* and maximum differences between the uninitialized 24 hour forecast (NIL) and the filtered forecast (DFI) for all prognostic variables were examined. When we compare these values to the differences at the initial time they are seen to be generally smaller. The changes made by DFI are to the high frequency components; since these are selectively damped during the course of the forecast, the two forecasts are very similar. After 24 hours the maximum difference in surface pressure is less than 1hPa and the *rms* difference is only 0.1hPa.

The basic measure of noise is the mean absolute value of the surface pressure tendency

$$N_1 = \left(\frac{1}{\mathrm{NMAX}}\right) \sum_{\mathrm{n}=1}^{\mathrm{NMAX}} \left|\frac{\partial p_s}{\partial t}\right| .$$

For well balanced fields this quantity has a value of about 1 hPa/3h. For uninitialized fields it can be an order of magnitude larger. In Figure 2 we plot the value of N_1 for three forecasts. The solid line represents the forecast

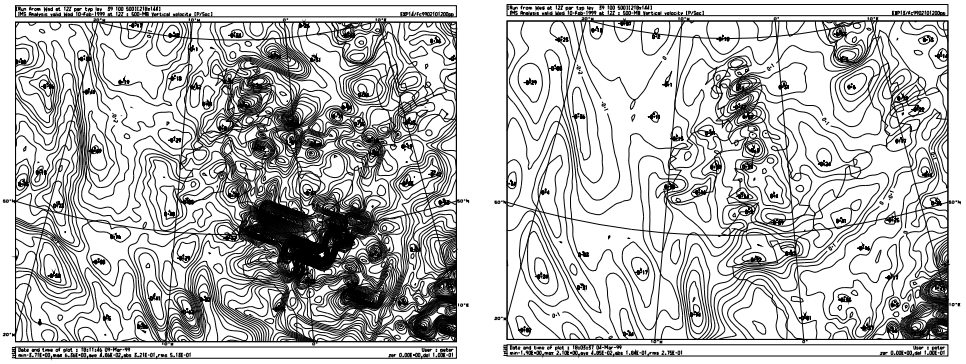

Figure 3. Vertical velocity at 500 hPa over western Europe and the eastern North Atlantic. (Left) Uninitialized analysis (NIL); (Right) after digital filtering (DFI).

from uninitialized data: we see that the value of N_1 at the beginning of the forecast is about 12 hPa/3h. This large value reflects the lack of an effective multivariate balance in the analysis. It takes about six hours to fall to a reasonable value. The dashed line is for a forecast starting from data initialized using the implicit normal mode method (NMI). The starting value is about 3 hPa/3h, falling to about 1.5 hPa/3h after twelve hours. The final graph (the dotted line) is for the digitally filtered data (DFI). The initial value of N_1 is now about 1.5, and remains more-or-less constant throughout the forecast. It is clear from this measure that DFI is more effective in removing high frequency noise than NMI.

The measure N_1 indicates the noise in the vertically integrated divergence field. However, even when this is small, there may be significant activity in the internal gravity wave modes. To see this, we look at the vertical velocity field at 500 hPa for the NIL and DFI analyses. The left panel in Fig. 3 shows the uninitialized vertical velocity field, zoomed in over western Europe and the eastern North Atlantic. There is clearly substantial gravity wave noise in this field. In fact, the field is physically quite unrealistic. The right panel shows the DFI vertical velocity. It is much smoother; the spurious features have been eliminated and the large values with small horizontal scales which remain are clearly associated with the Scottish Highlands, the Norwegian Mountains and the Alps. Comparison with the NMI method (see Lynch, *et al.*, 1999, for details) indicates that DFI is more effective than NMI in dealing with internal gravity wave noise. It is noteworthy that stationary mountain waves are unaffected by digital filtering, since they have zero frequency. This is a desirable characteristic of the DFI scheme.

8.3. BENEFITS FOR THE DATA ASSIMILATION CYCLE

In Lynch, *et al.*, 1999, a parallel test of data for one of the FASTEX intensive observing periods showed that the DFI method resulted in slightly

improved scores compared to NMI. As it is not usual for an initialization scheme to yield significant improvements in forecast accuracy, some discussion is merited. We cannot demonstrate beyond question the reason for this improvement. However, the comparative results showed up some definite defects in the implicit normal mode initialization as implemented in the reference HIRLAM model. It was clear that the NMI scheme did not eliminate imbalance at lower model levels. Moreover, although the noise level indicated by the parameter N_1 fell to a reasonable level in six hours, there was still internal gravity wave noise, not measured by this parameter. Any noise in the six hour forecast will be carried through to the next analysis cycle, and will affect the quality control and assimilation of new observational data. It is believed that the DFI scheme, with its superior ability to establish atmospheric balance, results in improved assimilation of data and consequently in a reduction of forecast errors.

9. Digital Filtering as a Constraint in 4DVAR

We conclude with a remark on the application of a digital filter as a weak constraint in four-dimensional variational assimilation (4DVAR). The idea is that if the state of the system is noise-free at a particular time, *i.e.*, is close to the slow manifold, it will remain noise-free, since the slow manifold is an invariant subset of phase-space. We consider a sequence of values $\{x_0, x_1, x_2, \cdots x_N\}$ and form the filtered value

$$\bar{x} = \sum_{n=0}^{N} h_n x_n. \tag{17}$$

The evolution is constrained, so that the value at the mid-point in time is close to this filtered value, by addition of a term

$$J_c = \frac{1}{2}\mu ||x_{N/2} - \bar{x}||^2$$

to the cost function to be minimized (μ is an adjustable parameter). It is straightforward to derive the adjoint of the filter operator. Gauthier and Thépaut (2001) applied such a constraint to the 4DVAR system of Météo-France. They found that a digital filter weak constraint imposed on the low-resolution increments efficiently controlled the emergence of fast oscillations while maintaining a close fit to the observations. As the values required for input to the filter are already available, there is essentially no computational overhead in applying this procedure. The dynamical imbalance was significantly less in 4DVAR than in 3DVAR. Fuller details may be found in Gauthier and Thépaut (2001).

10. Conclusion

The very notion of eliminating what is called "noise" is open to debate. There is no doubt as to the presence of high frequency motions in the at-

mosphere, and some evidence suggests that they may have a function in the development of meso-scale systems. If the feedback from HF components to the meteorologically significant motion is found to be important in certain circumstances, the application of filtering may be injudicious. It is important to minimize spurious imbalances in the analysed fields, through improved modelling of the multivariate background error covariances, and thus reduce the size of the changes induced by the initialization process. Removal of gravity waves cannot be unequivocally justified; the problem becomes all the more acute as model resolution increases.

References

Antoniou, A, 1993: *Digital Filters: Analysis, Design and Applications.* 2nd Edn., McGraw-Hill, 689pp.

Bubnová, Radmila, Gwenaëlle Hello, Pierre Bénard and Jean-François Geleyn, 1995: Integration of the fully elastic equations cast in the hydrostatic pressure terrain-following coordinate in the framework of the ARPEGE/Aladin NWP system. *Mon. Wea. Rev.*, **123**, 515–535.

Gauthier, P. and J. N. Thépaut, 2001: Impact of the digital filter as a weak constraint in the pre-operational 4DVAR assimilation system of Météo-France. *Mon. Wea. Rev.*, **129**, 2089–2102.

Hamming, R.W., 1989: *Digital Filters.* Prentice-Hall International, 284pp.

Huang, Xiang-Yu and Peter Lynch, 1993: Diabatic digital filtering initialization: application to the HIRLAM model. *Mon. Wea. Rev.*, **121**, 589–603.

Huang, Xiang-Yu and Xiaohua Yang, 2002. A new implementation of digital filtering initialization schemes for HIRLAM [`http://www.knmi.nl/hirlam/TechReports/TR53.pdf`]. HIRLAM Technical Report No. 53

Lynch, Peter and Xiang-Yu Huang, 1992: Initialization of the HIRLAM model using a digital filter. *Mon. Weather Rev.*, **120**, 1019–1034.

Lynch, Peter, 1997: The Dolph-Chebyshev Window: A Simple Optimal Filter. *Mon. Wea. Rev.*, **125**, 655-660.

Lynch, Peter, Dominique Giard and Vladimir Ivanovici, 1997: Improving the efficiency of a digital filtering scheme. *Mon. Wea. Rev.*, **125**, 1976–1982.

Lynch, Peter and Ray McGrath, 2001: Boundary Filter Initialization of the HIRLAM Model. Pp. 31–44 in *Advances in Mathematical Modelling of Atmosphere and Ocean Dynamics.* Ed. P. F. Hodnett. Kluwer Acad. Publ., 298pp.

Lynch, Peter, Ray McGrath and Aidan McDonald, 1999: Digital Filter Initialization for HIRLAM. HIRLAM Tech. Rep. No. 42 [`http://www.knmi.nl/hirlam/TechReports/TR42.ps.gz`].

Machenhauer, B., 1977: On the dynamics of gravity oscillations in a shallow water model with applications to normal mode initialization. *Beitr. Atmos. Phys.*, **50**, 253–271.

Oppenheim, A.V. and R.W. Schafer, 1989: *Discrete-Time Signal Processing.* Prentice-Hall International, Inc., 879 pp.

Raymond, W. H., 1988: High-order low-pass implicit tangent filters for use in finite area calculations. *Mon. Wea. Rev.*, **116**, 2132–2141.